



CHAPTER III EXPERIMENTAL

3.1 Materials

The materials used in this study were high-density polyethylene (HDPE), donated by Bangkok Polyethylene, and two grades of polystyrene (PS), purchased from Polysciences, as the matrix and dispersed phases, respectively. The properties of the polymers are given in Table 3.1. Both grades of the polystyrene resins were crushed to smaller pieces and their sizes were controlled by passing the flakes through a 425 μm sieve. All polymers were heated at 80°C under vacuum for 12 hours to eliminate any volatile substances. The polymer blend systems and their experimental temperatures are tabulated in Table 3.2.

Table 3.1 Properties of polymer blend components

Polymer	Suppliers	Grade	M_w^*	Melt Flow Index (g/10min)
PS1	Polyscience	Cat#23637	67,000	-
PS2	Polyscience	Cat#18544	62,000	-
HDPE1	Bangkok Polyethylene	1600J	68,000	14
HDPE2	Aldrich	Cat#42,801-9	-	42

* Quoted by the manufacturers

Table 3.2 Polymer blend systems

Blend system	Blend components (Drop/Matrix)	Temperature (°C)	Viscosity ratio (η_d/η_m)
A	PS1/HDPE1	143	2.6
B	PS2/HDPE1	155	0.5
C	PS1/HDPE2	139	1.0
A*	PS2/HDPE1	147	1.0

A* is system A of Cherdhirankorn et al¹¹

3.2 Rheological Characterization [Lerdwijitjarud et al. (2002)]

From the rheological properties in the previous work [Lerdwijitjarud et al. (2002)] the desired pairs of polymers and operating temperatures were selected for this study. The steady-state shear viscosity and the first normal stress difference of each polymer were measured by a cone-and-plate rheometer [Rheometric Scientific, model ARES] (25-mm plate diameter with cone angle 0.1 rad). The rheological properties were obtained at the shear rates ranged between 0.1 and 1 s⁻¹ using the rate sweep test mode, and the transient test mode was used when the shear rate was higher than 1 s⁻¹.

Table 3.3 Properties of polymer used in the previous work [Lerdwijitjarud et al. (2002)]

Polymer	Supplier	Grade	M _w	Melt Flow Index (g/10min)
Ps1	Aldrich	Cat#43011-0	162,000	14
PS2*	Polyscience	Cat#18544	62,000	-
PS3*	Polyscience	Cat#23637	67,000	-
HDPE1	Bangkok Polyethylene	2208J	73,000	10
HDPE2*	Bangkok Polyethylene	1600J	68,000	14

*Materials were selected for this work

Table 3.4 The Polymer blend systems in the previous work [Lerdwijitjarud et al. (2002)]

Blend system	Blend components	Temperature(°C)	Shear strain rate (s ⁻¹)	η _r	N _{1,r}
A1	PS1/HDPE1	220	7-70	0.85-1.00	0.50-0.91
A2	PS2/HDPE2	145	5-30	0.83-0.99	1.16-1.60
B1*	PS2/HDPE2	155	3-50	0.52-0.56	0.36-0.77
C1*	PS3/HDPE2	143	3-7	1.81-2.13	3.73-4.07
C2	PS3/HDPE2	145	2-3	1.89-1.98	3.08-3.21

* Polymer blend systems were selected for this work

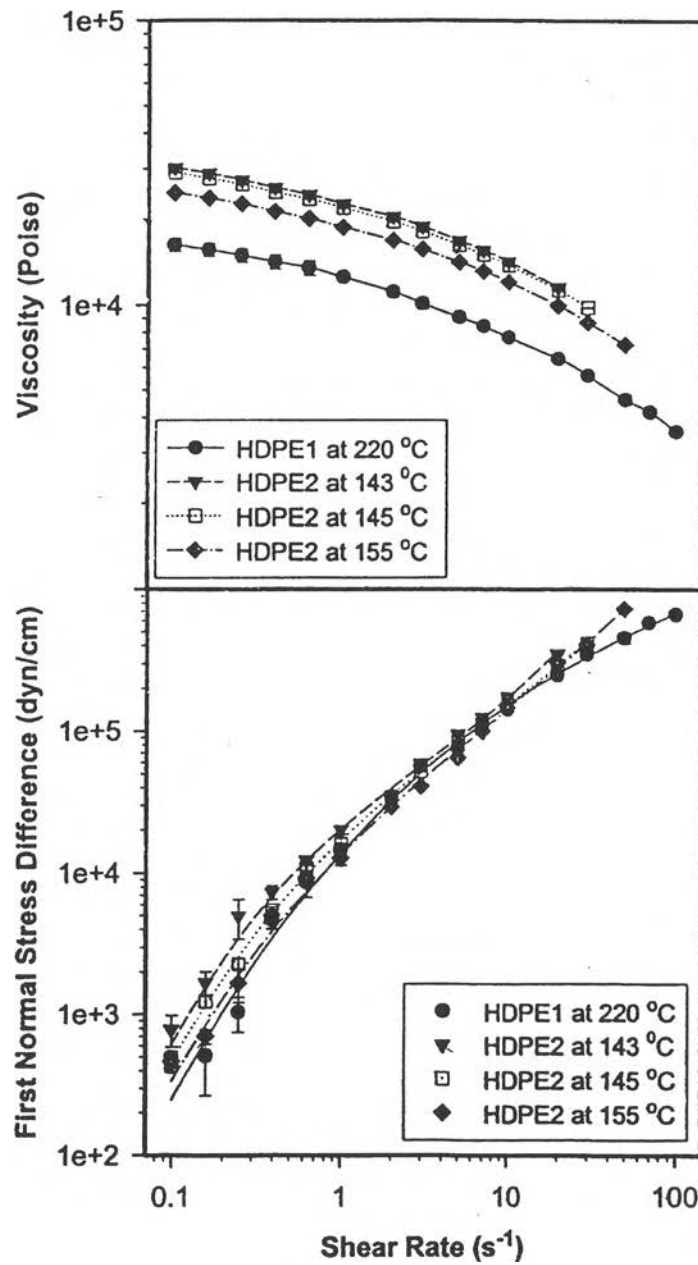


Figure 3.1 The dependence of (a) viscosity and (b) first normal stress difference ratio on shear rate of high density polyethylenes at various temperatures [Lerdwijitjarud et al. (2002)].

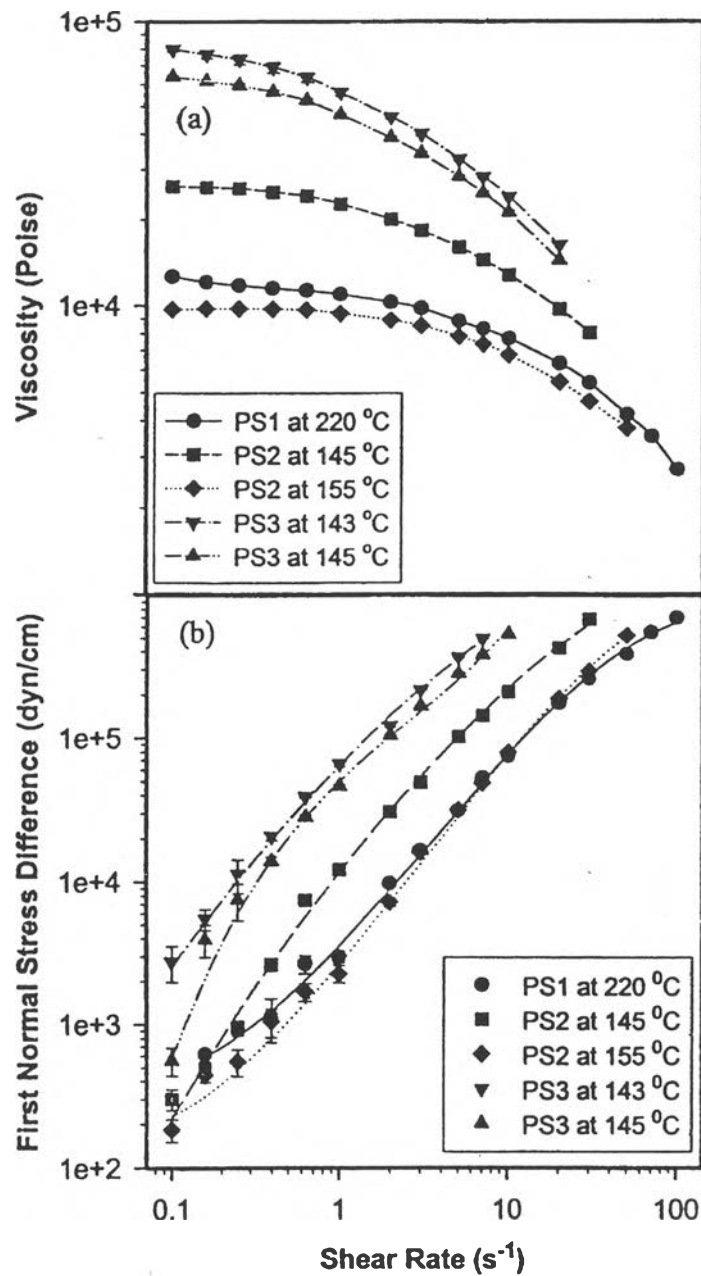


Figure 3.2 The dependence of (a) viscosity and (b) first normal stress difference on shear rate for polystyrenes at various temperature [Lerdwijitjarud et al. (2002)].

3.3 Observation of an Isolated Droplet in Shearing Flow

3.3.1 Shearing Apparatus

To generate simple shear flow and to observe the droplet behaviors, we used a flow cell device (Linkam CSS 450, Linkam Scientific Instruments Ltd., UK) with two quartz parallel disks attached to an optical microscope (Leica DMRPX, Leica Imaging Systems LTd., Cambridge, England). The images were recorded by a CCD camera (Cohu 4910, Cohu Inc., CA). They were analyzed on a computer using the Scion image software (<http://www.scioncorp.com>).

3.3.2 Sample Preparation

HDPE was molded in the form of disks 25-mm diameter and 0.5-1 mm thick by compression molding at 140°C with the pressure of 10 tons for 1 minute. Drops of PS were injected into the matrix by means of microsyringes, and covered with another HDPE disk to form a sandwich. The sandwich was placed on the bottom disk of the flow cell, covered with the top disk of the flow cell. The sample was held at the testing temperature.

3.3.3 Determination of Relaxation Time and Interfacial Tension

The sample was inserted between the two glass surfaces of the flow cell, whose roles were to maintain a constant specimen thickness and to ascertain that the imposed shear deformation was uniaxial. The sample was heated to the temperature chosen for the measurement. The desired strain was imposed onto a selected drop which moved the droplet out of the viewing window. The droplet then was allowed to completely relax back into a spherical shape during a period of at least 60 min, and then the droplet was subjected to the same strain in the opposite direction in order to bring the droplet back into the viewing window. Observation of retraction of the ellipsoidal droplet was carried out by using an optical microscope at a magnification depending on the drop-size. Around 100 to 200 droplet images were

record (10-20 second/frame). The deformation parameter, Def^* , of a retracting droplet vs. time was measured; it is known to decay exponentially [Luicinia et al. (1997)] from the proposed equation.

$$Def^* = Def^*_0 \exp [-t/\tau] \quad (3.1)$$

The slope of Def^* vs. t on a semi-log plot can be related to the characteristic relaxation time for a single drop, τ , and the interfacial tension calculated from the following relation;

$$\tau = \frac{(3 + 2\eta_r)(16 + 19\eta_r)r_o\eta_{m,o}}{40(1 + \eta_r)\Gamma} \quad (3.2)$$

To study the effect of droplet size on interfacial tension, the droplet size was varied from 70 μm to 400 μm at the fixed strain of 2 strain units and the effect of strain on the interfacial tension was then studied by varying strain from 1-8% with the fixed size of droplet at $370 \pm (10\mu\text{m})$. Figures 3.3 (a) and (b) show that the apparent interfacial tension values inferred from Eq. 3.2; it increases with the droplet size. The apparent interfacial tension obtained for large droplet is expected to be the most accurate which does not depend on strain; see Fig. 3.3. In principle, Eq. 3.2 is valid only for Newtonian systems, therefore interfacial tension for the polymerblend systems used in this work were taken from the literature [Brandrup and Immergut (1998)], which are 5.84 mN/m for system A at 143°C, 5.60 mN/m for system B at 155°C, 5.92 mN/m for system C at 139 °C, and 5.76 mN/m for system D at 147 °C.

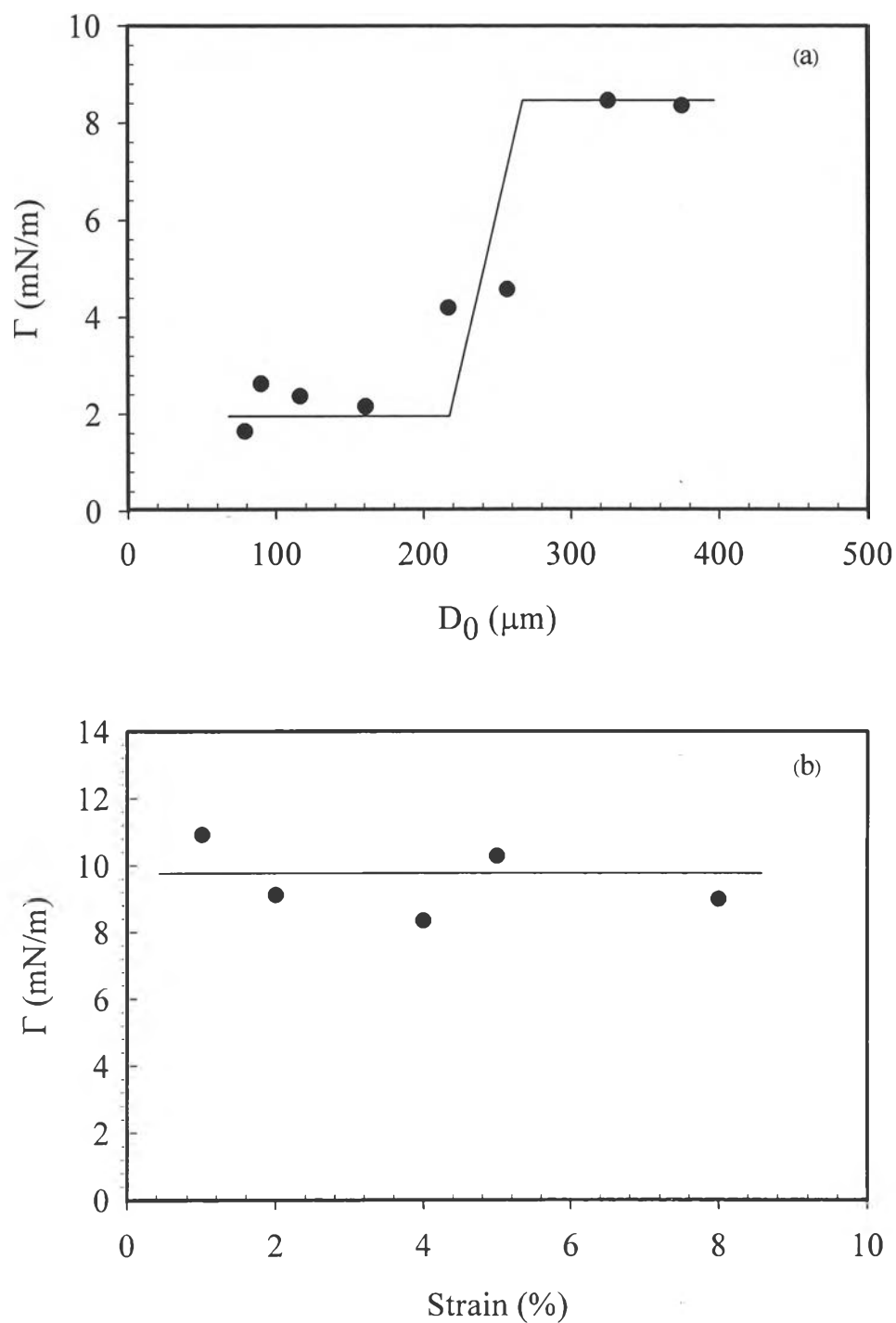


Figure 3.3 Dependence of the interfacial tension for system A: (a) on the applied initial droplet size (initial droplet size 78.4 μm - 386.5 μm at shear rate of 1 s^{-1} and fixed strain of 2 %); (b) on the applied strain (initial droplet size around $370 \pm (10) \mu\text{m}$ at shear rate of 1 s^{-1}).

Since the images of the deformed droplet were captured only in the plane perpendicular to the shear gradient direction, the true length of the principal axes of the ellipsoidal droplet could not be determined directly. The lengths of principle axes can be determined by using the orientation angle (θ), which is the angle of the major axis of the deformed droplet in the flow-flow gradient plane

Even if the lengths of the principal axes can be determined by using the method mentioned above, for convenience the lengths of the observable axes, shown in Fig 3.4 were used here to describe the behavior of each droplet by defining a modified deformation parameter Def^* as:

$$\text{Def}^* = (\mathbf{a}^* - \mathbf{c}) / (\mathbf{a}^* + \mathbf{c}) \quad (3.3)$$

where the asterisk denotes that the deformation parameter is an apparent one obtained from the droplet image projected into the flow-vorticity plane; see Fig 3.4.

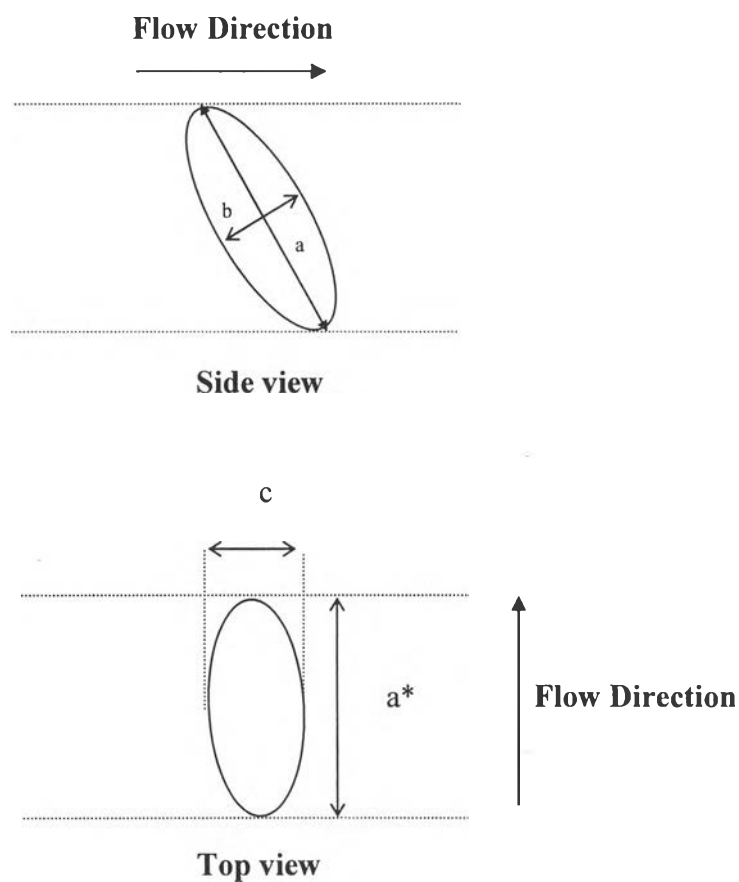


Figure 3.4 Schematic drawing of a single drop observed from the side and top views of the optical microscope; a and b are the long and short axes of the droplet in the flow-gradient plane, a^* is the a axis projected into the flow direction, and c is the principal axis in the radial direction.

3.3.4 Transient Deformation

The matrix phase was loaded into the flow cell and various single droplets were subsequently immersed into the matrix. The deformed shapes of the droplets were observed as a function of time from initial time until they attained steady-state shapes. Because of the limitation of flow cell device, a single droplet can not be imaged from the startup of shearing until attaining steady-state shape. Therefore the deformed shapes of isolated droplet could be determined by combining the results of several experiments. In the experiment of type 1, the droplet moved out

of viewing window through imposing low strain of less than 40 strain units (≈ 1 orbit) on the droplet. The droplet was left to relax its shape at least 60 minutes. Then the isolated droplet was imposed by the same strain but in the opposite direction which moved the droplet back into the viewing window, where we could image its deformation. However, the droplet could not be observed for large strain as it would move out of the viewing window. To obtain deformation of droplet at large strains, in the experiment of type 2, the droplet was imposed with a shearing flow continuously and images of the droplet were taken when the droplet passed through the viewing window. To clearly obtain droplet images, we stopped the flow each time the droplet reached the viewing window for a period of less than 1 second; this duration was relatively short for droplet to relax its shape by a significant amount. The time for one cycle of a droplet was recorded with a stopwatch along with the time shown on the Linksys program, and then the flow was imposed again until the droplet passed through the viewing window again. By repeating the experiment on droplets which were stopped at different times, we could assemble a consistent curve of deformation from the initial time to the time in which droplets attained steady-state shape. Transient experiments were achieved by varying the capillary number, Ca , from 5, 8, to 11 through varying droplet size at the same shear rate of 0.4 s^{-1} . To separate the effect of viscous force from the effect of elasticity, other experiments were carried out by keeping capillary number fixed at 8 and the elastic forces were varied by changing the shear rate from 0.10, 0.17, 0.40 to 0.63 s^{-1} and while using the droplet sizes of 289.7, 177, 85 and $56 \mu\text{m}$, respectively. Transient experiments for system B were carried out by keeping capillary number at 8 at the shear rate of 0.63 s^{-1} .

3.3.5 Steady-State Deformation and Breakup

The sample was loaded into the flow cell, droplet was left to relax to form spherical shapes for a period of at least 70 min; this was a little longer than the duration of the transient experiment because some droplets used here were larger. The steady-state shearing mode was used, steady-state shapes of isolated droplets below the critical capillary number for droplet breakup were determined. The critical

capillary number was determined by imposing successive changes of initial droplet size from small droplet size to larger droplet size at a fixed shearing rate at 0.4 s^{-1} for system A and system C and a fixed shearing rate at 0.63 s^{-1} for system B until the drop breakup was observed. To determine the steady-state droplet shape as a function of capillary number, the required strain to reach steady-state droplet shape depended on droplet size which increased with the droplet size. From the transient experiment, the required strain to reach steady-state droplet shape was determined and found to be around 4000 strain, at $Ca = 8$ and $D_0 = 85 (\pm 5 \mu\text{m})$. Therefore, a constant shear rate was then applied until a strain exceeding 4,000 strain units was attained. To ensure that the steady-state deformation had been attained, when a selected droplet passed through the viewing window, the droplet was imaged over a period of 5 to 10 min and we measured Def^* until its value became constant. After that, flow was stopped and the droplet shape relaxation was recorded with the CCD camera at speeds of 10-20 second per frame for approximately 90 minutes.

For droplets in which no steady-state shape was obtained, the unstable shapes of the droplets were recorded with time until the droplets were broken. The breakup processes for system A were achieved by keeping capillary number fixed at 11 using shear rates of 0.40 s^{-1} ; for system B capillary number was fixed at 9.5 and shear rates were $0.20, 0.63 \text{ s}^{-1}$.